Research Square

Preprints are preliminary reports that have not undergone peer review.
They should not be considered conclusive, used to inform clinical practice,
or referenced by the media as validated information.

Spinal Instrumentation Failure from the Perspective of Load Sharing

Takaya Kato (kato@crc.mie-u.ac.jp)
Mie University: Mie Daigaku https://orcid.org/0000-0003-1821-3197
Santo Ishikawa
Mie University Graduate School of Engineering Faculty of Engineering: Mie Daigaku Daigakuin Kogaku Kenkyuka Kogakubu
Tadashi Inaba
Mie University Graduate School of Engineering Faculty of Engineering: Mie Daigaku Daigakuin Kogaku Kenkyuka Kogakubu
Yuichi Kasai
Khon Kaen University Faculty of Medicine
Permsak Paholpak
Khon Kaen University Faculty of Medicine
Taweechok Wisanuyotin
Khon Kaen University Faculty of Medicine
Winai Sirichativapee
Khon Kaen University Faculty of Medicine
Weerachai Kosuwon
Khon Kaen University Faculty of Medicine
Kreingkrai Nabudda
Khon Kaen University Faculty of Engineering
Tetsutaro Mizuno
Seirei Hamamatsu Hospital: Seirei Hamamatsu Byoin

Research article

Keywords: biomechanics, lumbar spine, human cadaver experiment, spinal instrumentation, pedicle screw, intradiscal pressure, compression, strain, instrumentation failure

Posted Date: September 27th, 2021

DOI: https://doi.org/10.21203/rs.3.rs-900434/v1

License: This work is licensed under a Creative Commons Attribution 4.0 International License.
Loading [MathJax]/jax/output/CommonHTML/jax.js

Loading [MathJax]/jax/output/CommonHTML/jax.js

Abstract

Background

In recent years, pedicle screw (PS) fixation has often been used to stabilize the spine and correct deformities, yielding good clinical results. On the other hand, PS fixation is known to show problems such as instrumentation failure. However, few biomechanical studies have described causes of instrumentation failure. In this study, causes of instrumentation failure in lumbar PS fixation were investigated from the perspective of load sharing by measuring both strains generated in the rod and intradiscal pressure.

Methods

Four human cadaveric multi-segmental lumbar vertebrae (L2-L5) were used to prepare a control model and a PS fixation model. Next, axial compression tests were performed on each model using a universal material testing machine, and the strains generated in the rods and the intradiscal pressures were measured from strain gauges attached to the rods and a pressure sensor installed between L3-L4.

Results

Combined compressive and bending stresses were found to be generated in the rod, with bending stress around 10 times higher than compressive stress, and with vast differences in the levels of stress generated between right and left rods. Moreover, the stress shielding by PS fixation was small, and intervertebral discs were still subjected to a large load.

Conclusion

Preventing instrumentation failure in lumbar spine PS fixation, it seems necessary to strengthen the durability of the rod against bending stress and to ensure the stability of the anterior stabilizing element of the spine.

Introduction

In recent years, fixation surgeries that use pedicle screw (PS) fixation for gaining spinal stability and correcting spinal deformities have often been performed with good clinical outcomes [1–3]. PS fixation is known to encounter issues such as adjacent segment disease [4] and instrumentation failure [5]. Although a relatively high number of biomechanical findings have been obtained regarding causes of adjacent segment disease [6–9], very little biomechanical research has been reported on causes of instrumentation failure [10, 11]. The present study investigated causes of instrumentation failure in lumbar PS fixation from the perspective of load sharing by measuring both strain generated in the rods and intradiscal pressure during axial compressive loading of the spine.

Loading [MathJax]/jax/output/CommonHTML/jax.js

This research was conducted in the Department of Orthopaedics at Khon Kaen University, Thailand. The lumbar spines of four human cadavers donated to the Department of Anatomy at Khon Kaen University were resected by orthopedic surgeons at Khon Kaen University and cryopreserved at -30°C. The L2–L5 levels of these lumbar spines were used as test specimens. Ages at time of death were 65, 68, 81, and 89 years. Two cadavers were male and two were female. Death was due to heart disease in two cases and old age in two cases.

First, the human cadaveric lumbar spines were naturally thawed. After removing soft tissue such as muscle and fat, the PSs of the Suiren pedicle screw and rod system (KiSCO Co., Hyōgo, Japan) were inserted into L3 and L4 on a preparatory basis. In anticipation of severe degeneration of the lumbar spine, we prepared an injury model by excising the posterior portion of the intervertebral disks to a depth of about 5 mm using Luer forceps after complete excision of bilateral facet joints and the supraspinous and interspinous ligaments between L3 and L4. We used this injury model as a control model (Fig. 1a), considering that, when creating such an injury model, spinal alignment would be altered and biomechanical values such as intradiscal pressure would greatly change when compared with the intact model [12]. Then, we attached the rods between L3 and L4, being careful not to apply any mechanical load, and we used this as the PS-fixed model (Fig. 1b). Simple axial compression tests were performed on these two models for comparative investigation of strain generated in the rods and intradiscal pressure at these two models.

The E10000 (Instron, Grove City, PA, USA) universal testing machine was used as the testing machine. Both ends of the test specimens (L2 and L5) were grasped using a special fixing jig, then the specimens were fixed to the testing machine (Fig. 2). Afterwards, the initial load was set to zero, and axial compressive loading was applied at a load speed of 50 N/s until 700 N was reached, and the load was removed. Then, compressive loading was applied again under the same conditions, and the strain of the rods and the intradiscal pressure of the intervertebral disc were measured at 700 N during the second axial compressive load.

The measurements of 1) compressive stress and bending stress in the rods, 2) compressive load applied to the entire PS instrument, and 3) intradiscal pressure between L3 and L4 were obtained using the following methods.

First, to examine the compressive strain and bending strain generated in the rods, two strain gauges (KDGS; Kyowa Electronic Instruments Co., Tokyo, Japan) were attached to each rod, and strains were measured at four locations for anterior strain (ε_LA) and posterior strain (ε_LP) on the left rod, and anterior strain (ε_RA) and posterior strain (ε_RP) on the right rod (Fig. 3). Here, strain of the compressive components of the composite load (ε_comp) was calculated by applying each strain to Eq. 1, as half of the difference in absolute values of the anterior compressive strain (ε_A) and posterior tensile strain (ε_P):

Loading [MathJax]/jax/output/CommonHTML/jax.js

$$\epsilon_{comp} = \frac{\left|\epsilon_{\mathrm{A}}\right| - \left|\epsilon_{\mathrm{P}}\right|}{2} (1)$$

Then, based on the relationship between stress and strain shown in Eq. 2 [13], we obtained the stress of the compressive components (σ_comp) applied to the rods using the value of ε_comp:

$$\sigma_{comp} = E\epsilon_{comp} (2)$$

where E is Young's modulus for Ti-6Al-4V, the material used for the rods, defined in this experiment as E = 110 GPa (1.10×10^{11} N/m^2) [14].

Next, the bending strain (ε_bend) generated in rods can be obtained by subtracting the compressive strain (ε_comp) obtained in Eq. 1 from the absolute value for strain (ε_A). Bending strain (ε_bend) was thus obtained from Eq. 3:

$$\epsilon_{bend} = \left|\epsilon_{\mathrm{A}}\right| - \epsilon_{comp} (3)$$

The bending stress (σ_bend) applied to rods was then calculated using Eq. 4, similar to the stress in the compressive components (σ_comp):

$$\sigma_{bend} = E\epsilon_{bend} (4)$$

Moreover, the compressive load applied to the entire pedicle screw and rod system needs to be calculated to clarify the proportion of the 700 N vertical load applied to the specimen distributed to the vertebrae and spinal column fixture. Compressive load F applied to the rods was calculated using Eq. 5, and the sum of compressive forces [F] obtained from each of the left and right rods was used as the compressive force applied to the entire pedicle screw and rod system.

$$\mathrm{F} = \left(\sigma_{comp}\right) A (5)$$

where A in this equation indicates the cross-sectional area of the rod. The rod used in this experiment has A = 19.6 mm^2 (19.6×10^{-6} m).

Pressure sensors (A205-25; Nitta Corporation, Osaka, Japan) with a diameter of 9.5 mm and a thickness of 0.208 mm for the pressure-sensitive section were used to measure intradiscal pressure. After preparing the injury model, an incision was made with a scalpel in the lateral center portion of the intervertebral disks of L3 and L4 and the pressure sensor was inserted to a depth of approximately 2 cm. The signal detected by the sensor during compressive loads was thus amplified using an amplifier (amp box; Nitta Corporation). After A/D conversion using a PCD-320A sensor interface (Kyowa Electronic Instruments Co., Tokyo, Japan), load applied to the pressure sensor was stored as electronic data at a sampling frequency of 10 Hz. Intradiscal pressure (σ) (in megapascals) was calculated by dividing the load by the cross-

Loading [MathJax]/jax/output/CommonHTML/jax.js

Results

Table 1 shows the values of strain in the rods at a maximum load of 700 N for the PS-fixed model in the four test specimens. These data confirmed the generation of anterior compressive strain and posterior tensile strain in both left and right rods of the PS-fixed model, and that the absolute values of strain for both left and right rods were greater for the anterior region than for the posterior region. This indicated that the rods were subjected to a composite load of compression and bending (kyphosis). Table 2 shows the results of calculating compressive and bending stresses applied to the rods using these strain values. For these results, deformation of the spinal fixture was discovered to be heavily impacted by the bending load, with a large difference in stress levels seen between left and right rods.

Table 3 shows the sum of compressive loads generated in the left and right rods at a load of 700 N, corresponding to the compressive load applied to the entire PS instrument. These results showed the compressive load applied to the PS instrument was calculated to be a maximum of 281 N, a minimum of 110 N, and an average of 184.5 N, and an average of 26.3% of the 700 N load applied to each test specimen was distributed to the rods.

Table 4 shows the values of intradiscal pressure at a load of 700 N for each model in the four test specimens. Intradiscal pressure was discovered to be decreased when PS fixation was applied to the control model, and the rate of decrease was not very high, reaching a maximum of 40%, a minimum of 16%, and an average of 26.0%. Notably, the average rate of decrease in intradiscal pressure and the average compressive load applied to the PS instrument (Table 2) were approximately the same.

Discussion

The present results have biomechanical implications in considering causes of instrumentation failure following single-intervertebral PS fixation of the lumbar spine. That is, even under simple compressive loads, combined compressive and bending stresses are generated simultaneously in the rods, with bending stress an order of magnitude greater than compressive stress. In clinical cases, many instances of rod damage or breakage have been reported in association with long fusions such as scoliosis surgery, osteotomy, and total en bloc spondylectomy [15, 16]. In such cases, the rods were speculated to have been damaged or broken as a result of the extremely high bending stress applied.

Moreover, the present results showed that the stresses applied to the left and right rods are unequal, with a large difference between values. In addition to individual differences in test specimens, such as the shape of the vertebral body and spinal alignment, other possible causes are an asymmetrical angle of screw insertion, and in particular the fact that positioning the central axis of the specimens in the center of the testing machine is difficult because of its asymmetrical shape. However, the results of this study suggest that stresses on the left and right rods were asymmetrical despite the simple axial compression applied to the spine, with greater stress on one side of the rod. Considering only the prevention of rod damage and breakage, it seems important to use a strong design that prevents damage and breakage

Loading [MathJax]/jax/output/CommonHTML/jax.js

even if a load is applied to only a single rod. For example, such a design could correspond to increasing the thickness of the rods or using cobalt-chrome to make the rods, to provide sufficient resistance to bending stress [17].

Regarding the data on the rate of decrease in intradiscal pressure in this study, considerable variation was seen between test specimens, but the maximum rate of decrease was only 40% after PS fixation. Consequently, stress shielding by PS fixation was found to be not very significant, and intervertebral disks, as anterior elements, are still subjected to heavy loads. As a result, in clinical practice, if the anterior stabilizing elements of the spine are deemed unstable in single-intervertebral PS fixation, proper stabilization of the anterior stabilizing elements of the spine through the use of bone grafts or interbody cages appears critical for preventing instrumentation failure.

Furthermore, the average compressive load applied to the PS instrument and the average rate of decrease in intradiscal pressure obtained from the pressure sensors in this study were nearly equal, at approximately 26%. Consequently, the decrease in intradiscal pressure due to PS fixation appears to be replaced by an increase in the compressive load on the PS instrument. In other words, this result also appeared to clarify how the compressive load applied to the spine is distributed to the anterior stabilizing element and posterior PS instrument.

To investigate how the compressive load applied to the spine is distributed to anterior elements (vertebral body and intervertebral disks) and posterior elements (facet joints and PS), we believe that the question must be approached from the perspectives of both rod strain and intradiscal pressure, as in the present study.

Notable limitations of the present research were: 1) the small number of specimens; and 2) the fact that only simple axial compression loading tests were conducted. In future studies, we would like to increase the number of specimens, prepare a variety of models, and conduct both bending tests and rotation tests.

Conclusion

We applied simple compressive loads to human spine models in which highly unstable single-lumbar intervertebral segments were secured using PS fixation. We then measured changes in the strain of PS fixation rods and intradiscal pressure. The results showed that combined compressive and bending loads were generated in the rods, with 10 times more bending stress generated than compressive stress, and vast differences in the values of stresses were generated between left and right rods. Moreover, the stress shielding provided by PS fixation was small, meaning that a large load was still applied to the intervertebral disks. The key points to preventing instrumentation failure in single-lumbar intervertebral PS fixation thus seem to be the durability of the rod against bending stress, and the stability of the anterior stabilizing elements of the spine.

Abbreviations

Loading [MathJax]/jax/output/CommonHTML/jax.js

PS: Pedicle screw

Declarations

Acknowledgements

None

Funding

This work was supported by JSPS KAKENHI grant number JP20K04362.

Availability of data and materials

The datasets used and/or analyzed during the current study are available from the corresponding author on reasonable request.

Authors' contributions

TK and SI drafted the manuscript, did the first selection of articles, and assessed the quality of the papers. TI, PP, TW and KN gave important input for the method part of this paper, assessed the quality of the papers, and WS and WK revised the manuscript critically for its content. YK and TM helped to draft and correct the manuscript. All authors read and approved the final manuscript.

Competing interest

None

Ethics approval and consent to participate

This study was approved by the Ethics Committee for Human Research at Khon Kaen University (approval no. HE611293).

Consent for publication

Not applicable

References

Loading [MathJax]/jax/output/CommonHTML/jax.js

1. Cortesi Paolo A, Assietti Roberto C, Fabrizio P, Domenico P, Mauro C, Paolo T, Patrizia V, Roberto C, Davide B, Stefano C, Giancarlo M, Lorenzo G. Epidemiologic and Economic Burden Attributable to First Spinal Fusion Surgery. Spine. 2017;42(18):1398–404.
2. Yasuaki Imajo T, Taguchi K, Yone A, Okawa K, Otani T, Ogata H, Ozawa Y, Shimada M, Neo T Iguchi., 2015. Japanese 2011 nationwide survey on complications from spine surgery. J Orthop Sci. 20, 38–54.
3. Caroline P, Thirukumaran B, Raudenbush Y, Li R, Molinari P, Rubery AM. National Trends in the Surgical Management of Adult Lumbar Isthmic Spondylolisthesis: 1998 to 2011. Spine. 2016;41:490–501.
4. HashimotoãK A 1, Kanno T, Itoi H E. Adjacent segment degeneration after fusion spinal surgery—a systematic review. Int Orthop. 2019;43:987–93.
5. Jutte PC, Castelein RM. Complications of pedicle screws in lumbar and lumbosacral fusions in 105 consecutive primary operations. Eur Spine J. 2002;11(6):594–8.
6. Panjabi M, Henderson G, James Y, Timm JP. StabilimaxNZ® versus simulated fusion: evaluation of adjacent-level effects. Eur Spine J. 2007;16:2159–65.
7. Dahl MC, Ellingson AM, Mehta HP, Huelman JH, Nuckley DJ. The biomechanics of a multilevel lumbar spine hybrid using nucleus replacement in conjunction with fusion. Spine J. 2013;13:175–83.
8. Khoddam-Khorasani P, Arjmand N, Shirazi-Adl A. Trunk hybrid passive-active musculoskeletal modeling to determine the detailed T12–S1 response under in vivo loads. Ann Biomed Eng. 2018;46:1830–43.
9. Azadi A, Arjmand N. 2021. A comprehensive approach for the validation of lumbar spine finite element models investigating post-fusion adjacent segment effects. J Biomech 121, 110430. doi: 10.1016/j.jbiomech. 110430.
10. Chen CS, Chen WJ, Cheng CK, Jao SH, Chueh SC, Wang CC. Failure analysis of broken pedicle screws on spinal instrumentation. Med Eng Phys. 2005;27(6):487–9. doi:10.1016/j.medengphy.2004.12.007.
11. Luca A, Ottardi C, Sasso M, Prosdocimo L, La Barbera L, Brayda-Bruno M, Galbusera F, Villa T. Instrumentation failure following pedicle subtraction osteotomy: the role of rod material, diameter, and multi-rod constructs. Eur Spine J. 2017;26(3):764–70. doi:10.1007/s00586-016-4859-8.
12. Zahari SN, Latif MJA, Rahim NRA, Kadir MRA, Kamarul T. 2017. The Effects of Physiological Biomechanical Loading on Intradiscal Pressure and Annulus Stress in Lumbar Spine: A Finite Element Analysis. J Healthc Eng. 2017, 9618940. doi: 10.1155/2017/9618940.
13. Timoshenko SP, Goodier JN. Theory of Elasticity. New York: McGraw-Hill; 1970. pp. 6–7.
14. Park JB. Biomaterials Science and Engineering. New York: Plenum Press; 1984. p. 215.
15. Park SJ, Lee CS, Chang BS, Kim YH, Kim H, Kim S, Chang SY, Korean Spine Tumor Study Group. Rod fracture and related factors after total en bloc spondylectomy. Spine J. 2019;19(10):1613–9. doi:10.1016/j.spine.2019.04.018.

Loading [MathJax]/jax/output/CommonHTML/jax.js

16. Zhao J, Li B, Chen Z, Yang C, Li M. Rod fracture after long construct fusion in adult spinal deformity surgery: A retrospective case-control study. J Orthop Sci. 2019;24(4):607–11. doi: 10.1016/j.jos.2018.12.010. Epub 2019 Jan 3.
17. Jazini E, Gelb DE, Tareen J, Ludwig SC, Harris JA, Amin DB, Wang W, Van Horn MR, Patel PD, Mirabile BA, Bucklen BS. 2021. Comprehensive In Silico Evaluation of Accessory Rod Position, Rod Material and Diameter, Use of Cross-connectors, and Anterior Column Support in a Pedicle Subtraction Osteotomy Model: Part II: Effects on Lumbosacral Rod and Screw Strain. Spine (Phila Pa 1976). 46(1), E12-E22.

Tables

Table 1

Values of strain at each position of the rod at a maximum load of 700 N for the PS-fixed model of the four test specimens from strain gauges.

	Anterior		Posterior	
	ε_{LA} ($\times 10^{-6}$)	ε_{RA} ($\times 10^{-6}$)	ε_{LP} ($\times 10^{-6}$)	ε_{RP} ($\times 10^{-6}$)
Test body 1	-1040	-995	875	900
Test body 2	-913	-1180	853	1028
Test body 3	-1070	-1020	1058	923
Test body 4	-405	-595	390	508

Table 2

Result of calculation of compressive and bending stresses applied to the rods using values from Table 1.

Loading [MathJax]/jax/output/CommonHTML/jax.js

	Compressive stress (σ_{comp})		Bending stress (σ_{bend})	
	Left (MPa)	Right (MPa)	Left (MPa)	Right (MPa)
Test body 1	9.08	5.23	105	104
Test body 2	3.30	8.36	97.1	121
Test body 3	0.66	5.34	117	107
Test body 4	0.83	4.79	43.7	60.7

Table 3

Sums of compressive loads generated in the left and right rods at a load of 700 N.

	Rt rod (N)	Lt rod (N)	Load (N)
Test body 1	178.2	102.5	280.8
Test body 2	64.8	164.1	228.9
Test body 3	13.0	104.8	117.7
Test body 4	16.2	94.0	110.2

Table 4

Intradiscal pressure at a load of 700 N for each model in the four test specimens from pressure sensors.

Loading [MathJax]/jax/output/CommonHTML/jax.js

	Control (MPa)	PS-fixed (MPa)
Test body 1	0.99	0.81
Test body 2	0.70	0.59
Test body 3	0.88	0.53
Test body 4	1.14	0.82

Figures

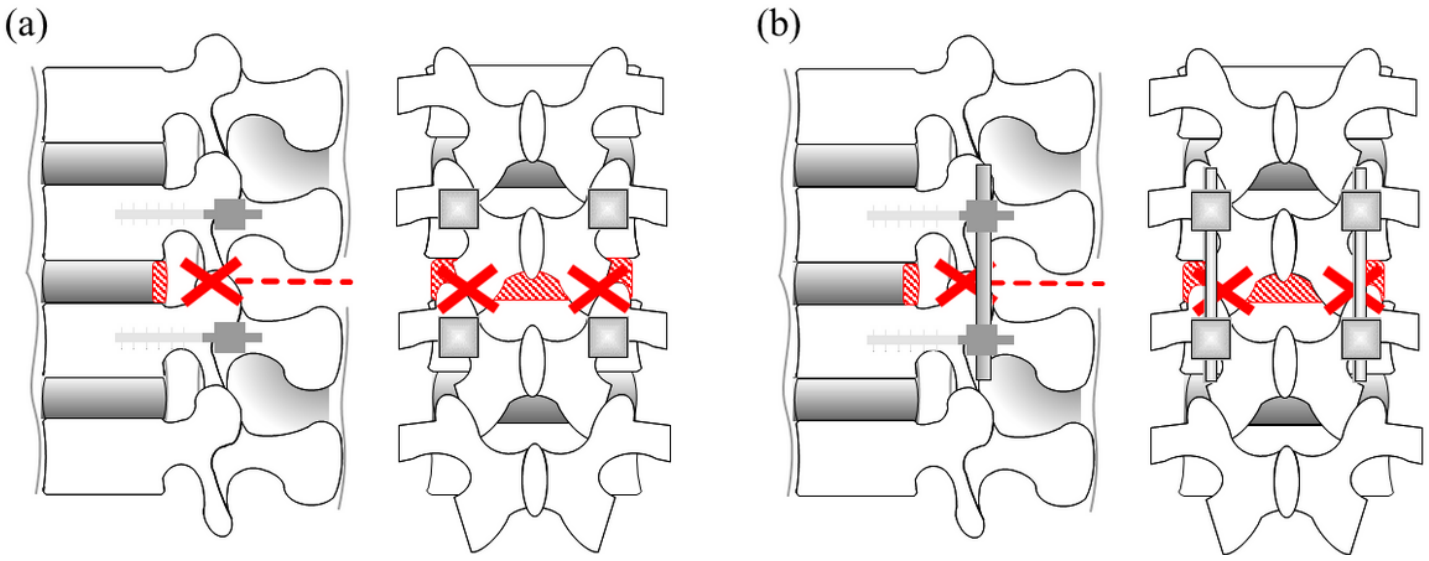

Figure 1

Schematic illustrations of test models. a) Control model. b) PS-fixed model. Excision sites are shown as crosses (facet joints) and dashed lines (supraspinous and interspinous ligaments). The excised portion of intervertebral disc is shown as the red shaded area

Loading [MathJax]/jax/output/CommonHTML/jax.js

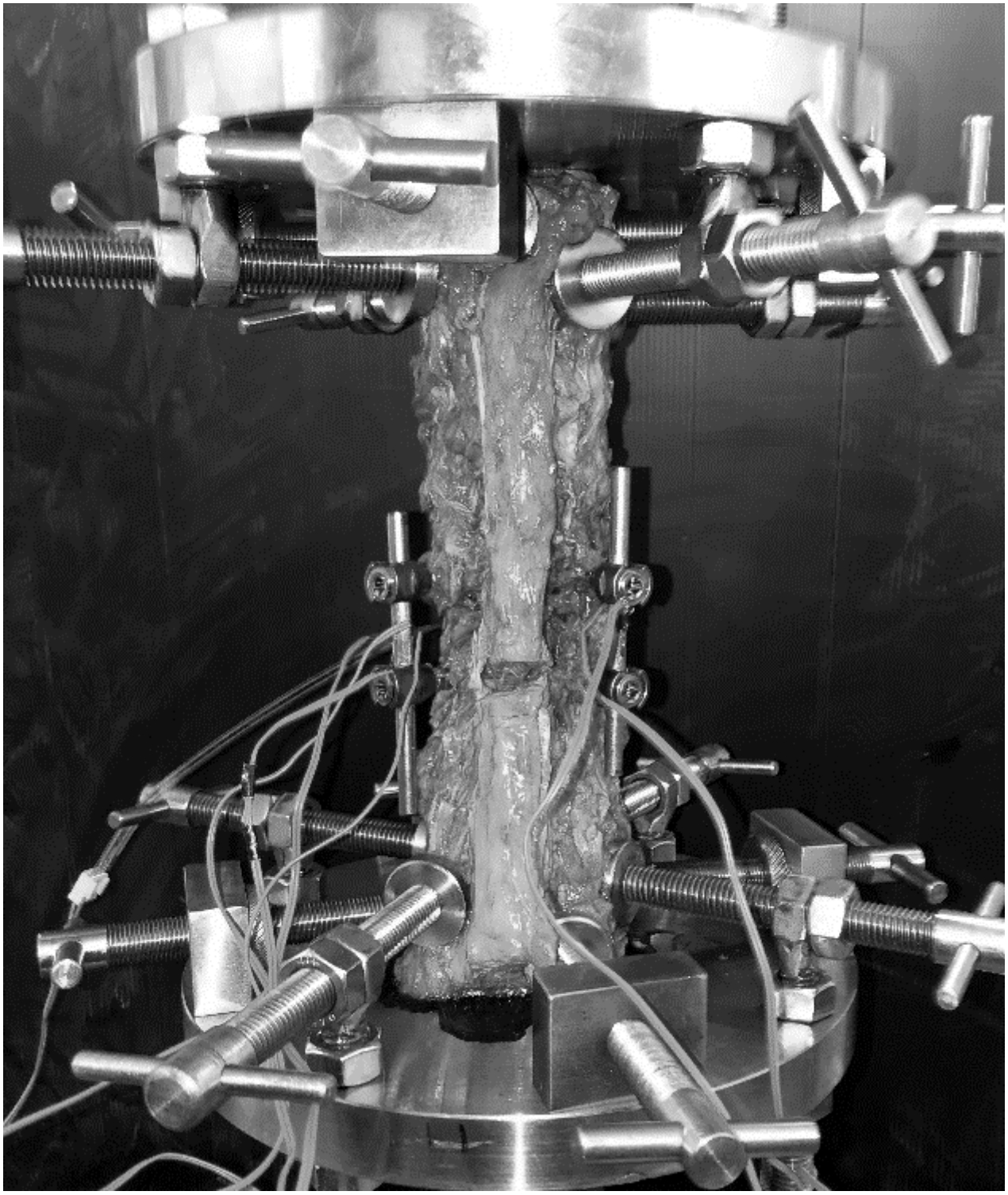

Figure 2

Fixation of a human cadaveric lumbar spine to the tester

Loading [MathJax]/jax/output/CommonHTML/jax.js

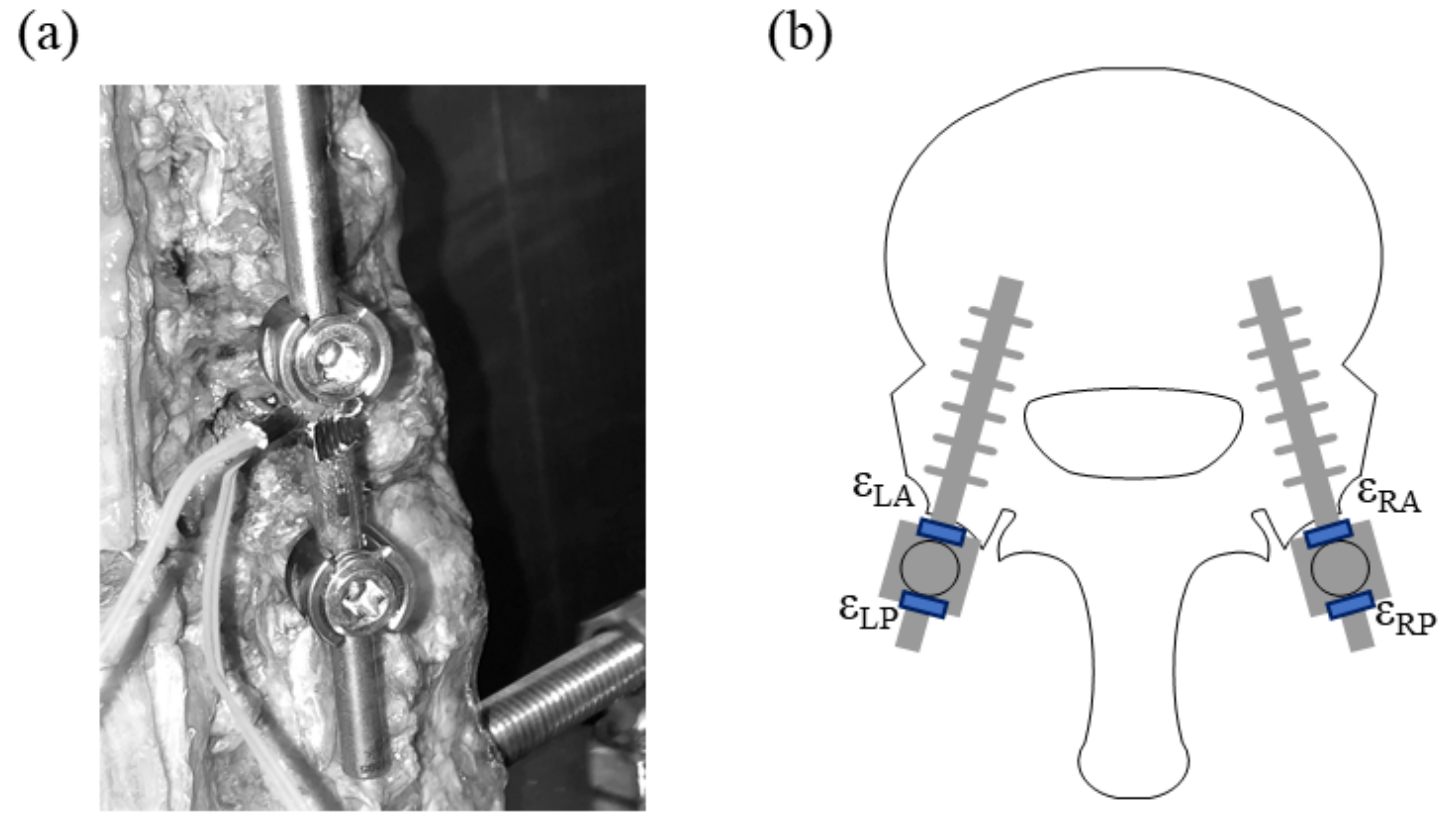

Figure 3

Sites of strain gauge installation. a) Strain gauges installed on the rod. b) Schematic illustration of positions of strain gauge attachment. The strain gauges are installed on the anterior and posterior sides of the rod.

Loading [MathJax]/jax/output/CommonHTML/jax.js